

Spectroscopy of metallic and insulating V_2O_3

O. Müller, J. P. Urbach, E. Goering, T. Weber, R. Barth, H. Schuler, M. Klemm, and S. Horn
Experimentalphysik II, Universität Augsburg, Memminger Strasse 6, 86159 Augsburg, Germany

M. L. denBoer

Hunter College of CUNY, 695 Park Avenue, New York, New York 10021

(Received 21 April 1997; revised manuscript received 8 August 1997)

V_2O_3 exhibits as a function of temperature a metal-insulator transition (MIT) associated with a structural and a magnetic transition, which we have studied with x-ray-absorption measurements of V_2O_3 at the V $2p$ and O $1s$ edge as well as photoemission measurements above and below the MIT. The O $1s$ edge shifts ~ 0.3 eV to lower energy in the metallic phase and the linear dichroism is enhanced in the insulating state, an enhancement discussed in a molecular-orbital picture. These effects are independent of whether the insulating state is achieved by cooling, Cr doping, or stress. We conclude the monoclinic distortion plays only a minor role in the MIT; the major factor is the change in the c/a ratio. The V $2p$ edge is much narrower in the insulating phase, perhaps due to changes in electron phonon coupling. [S0163-1829(97)05148-5]

INTRODUCTION

The metal-insulator transition in vanadium oxides is a long-standing and yet unsolved issue. The metal-insulator transition (MIT) may occur as a function of temperature, pressure, or doping. In pure V_2O_3 the transition occurs at $T_{MI}=170$ K and involves a change from a high-temperature paramagnetic metallic phase to an antiferromagnetically ordered insulating phase and is associated with a structural transformation. The trigonal (corundum) symmetry of the metallic phase reduces to monoclinic at low temperature. As is customary, we describe the monoclinic structure using distorted pseudohexagonal lattice vectors $(a_1a_2a_3,c)$ rather than the monoclinic lattice vectors. The trigonal structure includes V-V pairs perpendicular to the basal (0001) plane.

In a simplifying picture of the monoclinic distortion,¹ the V-V pairs lengthen and tilt by $\sim 1.8^\circ$ with respect to the basal plane. This tilt lengthens one basal plane V-V distance, while the other two would shorten were it not for a compensating lengthening of the lattice as a whole in the appropriate direction in the basal plane. To keep the average V-O distance almost unchanged, the O octahedra surrounding the V pairs become skewed, leading to the tilt of the c axis associated with the monoclinic distortion. Although the vertical V-V pair distance lengthens, the c axis is actually shorter. This and the aforementioned lengthening in the basal plane in one direction reduces the unusually high c/a ratio of 2.840 in the metallic trigonal phase to 2.808 in the monoclinic phase.

Doping with chromium, which substitutes for vanadium to produce $(V_{1-x}Cr_x)_2O_3$, leads to a phase that is insulating even at room temperature for $x \geq 0.04$. The c/a ratio is even smaller than in the monoclinic phase of pure V_2O_3 . However, all the vertical (along c) V-V pair distances are larger and the trigonal symmetry is preserved. The Cr-doped phase is paramagnetic at room temperature. Only at lower temperatures does magnetic ordering occur; below 180 K an antiferromagnetic monoclinic phase forms.

The MIT in both pure and doped V_2O_3 has been discussed

in terms of a Mott-Hubbard transition, especially since vanadium deficiency, which amounts to hole doping, causes the development of an incommensurate spin-density wave, in agreement with the theoretical phase diagram of a Mott-Hubbard insulator. Possible cause-and-effect relationships between the structural changes and the electronic and magnetic transitions are important to understanding the mechanism of the MIT. We have used x-ray absorption and photoemission spectroscopy to study the electronic structure of pure V_2O_3 above and below T_{MI} as well as oriented insulating trigonal thin films of pure and Cr-doped V_2O_3 . We find that, although they are structurally different, the electronic structure of the trigonal thin films and low-temperature monoclinic insulating V_2O_3 is essentially the same, and all three differ in similar ways from the metallic phase. We conclude that the important factor in the MIT is not the symmetry breaking, but rather an increase in the trigonal distortion.

The electronic structure of V_2O_3 has been described by Goodenough² using a molecular-orbital (MO) model. This predicts V $3d$ bands with three distinct symmetries: (1) e_g^π orbitals between V pairs in the basal plane; (2) a_{1g} orbitals between V pairs along c ; and (3) e^σ orbitals with components both perpendicular and parallel to c . In the metallic phase the e_g^π and a_{1g} orbitals overlap (are essentially degenerate) and cross ϵ_F , while the e^σ orbitals are located several eV above ϵ_F . In the insulating phase the e_g^π and a_{1g} orbitals no longer overlap, and in addition the degeneracy of the in-plane e_g^π orbitals is lifted due to the breaking of the threefold symmetry in the basal plane. A gap develops; the filled and empty bands closest to ϵ_F are hybridized e_g^π and a_{1g} . Antiferromagnetic ordering then follows directly as a natural consequence of the filled bands in the insulating state.³ Consistent with this MO model, later work implies the unoccupied bands above ϵ_F have primarily V $3d$ character.⁴ A Hubbard on-site repulsion, while not a consequence of the model, could contribute to the gap, and the split a_{1g} bands may be designated as upper and lower Hubbard bands. The MO

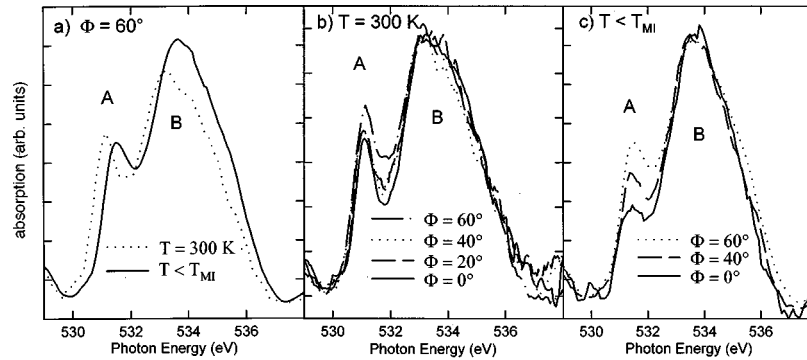


FIG. 1. The O K x-ray-absorption edge of the (0001) basal plane of V_2O_3 under various conditions. (a) compares V_2O_3 in the metallic ($T=300$ K) and insulating ($T < T_{MIT}$) state, and (b) and (c) show the dependence of each on the angle Φ between the polarization vector and the surface normal.

model does not take into account how V $3d$ -O $2p$ hybridization could be affected by the structural rearrangements associated with the MIT.

Photoemission has been used to study the occupied states of V_2O_3 , both polycrystalline⁵ and the cleaved (10 $\bar{1}$ 2) surface,⁶ until recently⁷ the only atomically smooth surface available. Single-crystal measurements are important as they provide much more detailed information in this anisotropic compound. The measurements showed a V $3d$ region separated by a few eV from a broader primarily O $2p$ region, with no distinct gap between these regions. In studying the reactivity of V_2O_3 , a very important issue in catalysis, it was found that SO_2 reacts only weakly with the (10 $\bar{1}$ 2) surface.⁸ This is surprising as SO_2 reacts strongly with the same surface of chemically similar Ti_2O_3 .⁹ Angle-resolved photoemission revealed broad features and little bulk band dispersion,¹⁰ in contrast to theoretical predictions.¹¹ Resonant photoemission of the V $3d$ level was strongly anisotropic, displayed a delayed onset, and, surprisingly, appeared to correlate with emission from the O $2p$ level.¹² A photoemission study of the MIT, again on the (10 $\bar{1}$ 2) surface, showed the opening of a gap in the insulating state for both pure and Cr-doped V_2O_3 .¹³ The unoccupied states in polycrystalline V_2O_3 at room temperature have been studied with near-edge x-ray absorption by de Groot *et al.*,^{14,15} who described the V $2p$ (L_{II} and L_{III}) edges in terms of atomic transitions including crystal-field splittings. The O $1s$ (K) edge should reflect the amount of states of p character (with respect to O sites) admixed into the unoccupied bands above ϵ_F .

EXPERIMENT

Bulk single crystals were prepared by chemical transport of V_2O_3 powders using $TeCl_4$ as transport agent and were characterized by resistivity measurements and Laue x-ray diffraction. Thin films of V_2O_3 and Cr-doped V_2O_3 were grown by evaporation, in the presence of O_2 , on sapphire substrates.¹⁶ We can produce pure metallic or insulating V_2O_3 films by varying the growth conditions. Within the resolution of our x-ray diffraction measurements insulating pure films are structurally identical to metallic films or the bulk crystal, except for larger basal plane lattice parameters, which means such films experience ‘‘negative pressure’’ in

this plane.¹⁶ Before the spectroscopic measurements, samples were characterized *in situ* by low-energy electron diffraction (LEED); all exhibited sharp trigonal LEED patterns characteristic of the basal (0001) plane. Our spectra change markedly at the MIT, as described below, confirming that these surface-sensitive measurements reflect the bulk properties of V_2O_3 .

X-ray spectroscopy used monochromator PM5 (HE-PGM3) of the Berlin electron storage ring BESSY I. Photons of the appropriate energy can cause transitions from the O $1s$ and V $2p$ states into unoccupied states at the absorbing atomic species. The dipole selection rules imply that for the O $1s$ (V $2p$) edge these unoccupied states will have p (d) character with respect to O (V) sites. The synchrotron radiation is linearly polarized, and the use of oriented single crystals and thin films makes it possible to measure spectra with various orientations of the crystal axes with respect to the polarization direction. The x-ray-absorption coefficient was measured by monitoring the total electron yield, which is somewhat surface sensitive. Photoemission measurements were carried out at beam line U4A of the National Synchrotron Light Source at Brookhaven National Laboratory. In contrast to x-ray absorption, photoemission is sensitive to changes in the occupied electronic states. Combined, the two techniques allow a rather complete view of the electronic structure. By measuring in both the metallic and insulating phases, we can observe those changes associated with the MIT.

RESULTS AND DISCUSSION

Figure 1 displays O $1s$ x-ray-absorption spectra of single-crystal V_2O_3 under various conditions. The polarization vector forms an angle of 60° with respect to the surface normal, the [0001] c axis, as mentioned above. Including the effects of hybridization in the MO model discussed above,² the lower-energy (~ 531 eV) peak A in Fig. 1 is due to the O p admixture to the e_g^π and a_{1g} states, while the higher-energy (~ 533.5 eV) peak B is due to the O p admixture to the e_g^σ states. Figure 1(a) shows that when V_2O_3 becomes insulating, peaks A and B both shift about 0.3 eV to higher energy. In addition, the intensity ratio B/A increases, implying that in the insulating state the hybridization of the unoccupied O $2p$ states with the V $3d$ (e_g^π and a_{1g} ; peak A) states de-

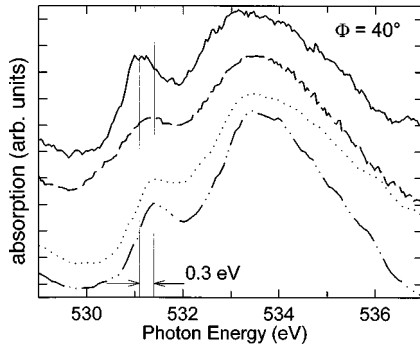


FIG. 2. Comparison of the O K x-ray-absorption edge of V_2O_3 samples. The solid (dash-dotted) line is the spectrum of bulk V_2O_3 in its metallic (insulating) state, the dotted line is the spectrum of an insulating Cr-doped V_2O_3 thin film, and the dashed line is the spectrum of an insulating trigonal V_2O_3 thin film. As indicated, the first peak in all spectra is shifted by 0.3 eV with respect to that of bulk metallic V_2O_3 .

increases relative to their hybridization with the V $3d$ (e^σ ; peak B) states.

The angular dependence reveals more about the orbitals involved in the transition. With the polarization vector \mathbf{E} of the incident radiation parallel to the c axis, peak A measures the O $2p_z$ contribution to the predominantly V $3d$ e_g^π and a_{1g} bands and peak B the O $2p_z$ contribution to the e^σ band. With \mathbf{E} in the basal plane, the O $2p_{x,y}$ contribution to each of these V bands is detected. Anisotropy in the angular dependence of the spectral features indicates anisotropy in the V $3d$ -O $2p$ hybridization.

In Figs. 1(b) and 1(c) we show spectra of V_2O_3 above and below T_{MI} for different angles Φ of \mathbf{E} relative to the $[0001]c$ axis. (We note parenthetically that the spectra do not depend on the orientation of the polarization vector within the basal plane, as expected due to the near isotropy of the crystal within this plane.) As \mathbf{E} is rotated out of the basal plane ($\Phi=0^\circ$ to $\Phi=60^\circ$), peak A increases slightly relative to peak B in the metallic phase, and much more in the insulating phase. The smaller anisotropy in the metallic phase reflects the near degeneracy of the a_{1g} and e_g^π states in this phase suggested by Goodenough.² This near degeneracy is lifted in the insulating phase, making it more anisotropic.

In Fig. 2 the O $1s$ x-ray-absorption spectrum of a bulk V_2O_3 single crystal in its metallic and insulating state is compared to that of two trigonal thin films, insulating pure V_2O_3 and insulating Cr-doped V_2O_3 . In all spectra, the polarization vector \mathbf{E} is 40° from the $[0001]$ surface normal. The spectra of both insulating thin films are similar to that of the bulk single crystal in its insulating phase. Specifically, the lower-energy peak A , corresponding to the O contribution to the a_{1g} and e_g^π states, is shifted to higher energy and has less weight relative to peak B than in the metal, and the angular dependence (not shown) resembles that of the bulk single crystal in the insulating state. Evidently, the differences between the spectra of metallic and insulating materials are independent of whether the insulating state is achieved by Cr doping, lowering the temperature, or the ‘‘negative pressure’’ of the thin films. Moreover, the differences do not depend on the lattice symmetry, since, as noted, the insulating bulk single crystal is monoclinic, while both thin films

are trigonal, differing from the also trigonal bulk metallic crystal only in that their c/a ratio is smaller.

The observed similarities in the spectra of both trigonal and monoclinic materials, including the thin films, which, as mentioned, are trigonal, elucidates the relative importance of the structural changes associated with the MIT. A decrease in the c/a ratio further distorts the VO_6 octahedra away from cubic symmetry, inducing into the ligand crystal field a trigonal field component that tends to split the a_{1g} and e_g^π states.² In the trigonal metallic phase the distortion of the VO_6 octahedra is small, so the trigonal component is too weak to entirely remove the degeneracy of the a_{1g} and e_g^π states. In the insulating phase, the trigonal component strengthens, lifting the degeneracy of the a_{1g} and e_g^π states, which are then anisotropic and produce the strong anisotropy of the O $1s$ peak A observed in the insulating state. The determining parameter for the changes is then the degree of trigonal distortion of the oxygen octahedron, or equivalently the change in the c/a ratio. On the other hand, the monoclinic symmetry-breaking distortion, i.e., the tilting of neighboring V atoms with respect to the trigonal c axis, which occurs in pure V_2O_3 at the MIT, may not be essential to achieving the insulating state, but could be a purely electrostatic effect, as also suggested for the tilt of V-V pairs in VO_2 .¹⁷

Magnetic ordering appears to play no role either in the MIT or on the local electronic structure. This is in agreement with the MO model,² in which, as mentioned above, magnetic order is simply a consequence of the filled bands present in the insulating state, and supported by our measurements, which show no differences, in particular, nonattributable to magnetic ordering: The spectra of the V_2O_3 single crystal in its monoclinic insulating state, which is antiferromagnetically ordered, are very similar to those of the paramagnetic trigonal Cr-doped thin film. Nor do the spectra of the film change when the temperature is lowered and it becomes a monoclinic antiferromagnet (not shown).

Our conclusion that the decisive factor in the MIT is the increased distortion of the VO_6 octahedra achieved by the decrease in c/a ratio, not the symmetry breaking, is supported by recent V K -edge extended x-ray-absorption fine structure (EXAFS) measurements, which suggest local or dynamic monoclinic distortion of the V_2O_3 lattice is present already in the nominally trigonal metallic phase, although less than in the insulating phase.¹⁸ The MIT could then be associated with a transition from short- to long-range order, so that below T_{MI} the global symmetry is broken, producing the monoclinic cell observed in x-ray diffraction. If local monoclinic distortion is present in both the metallic and the insulating phase, it cannot be decisive to the MIT, which must rather be driven by the increased distortion of the VO_6 octahedra caused by the decrease in c/a ratio. The changes in anisotropy we observe can be satisfactorily explained by a change in the local environment of the oxygen atoms, which, as just discussed, need not involve a change in the site symmetry, but rather an increase in an already present distortion. The similarity of the spectra of Cr-doped and bulk insulating V_2O_3 could then also be due to local monoclinic distortion in the Cr-doped sample, a possibility that could be studied by EXAFS.

It is difficult to assign peaks in the V $2p$ spectra, shown in

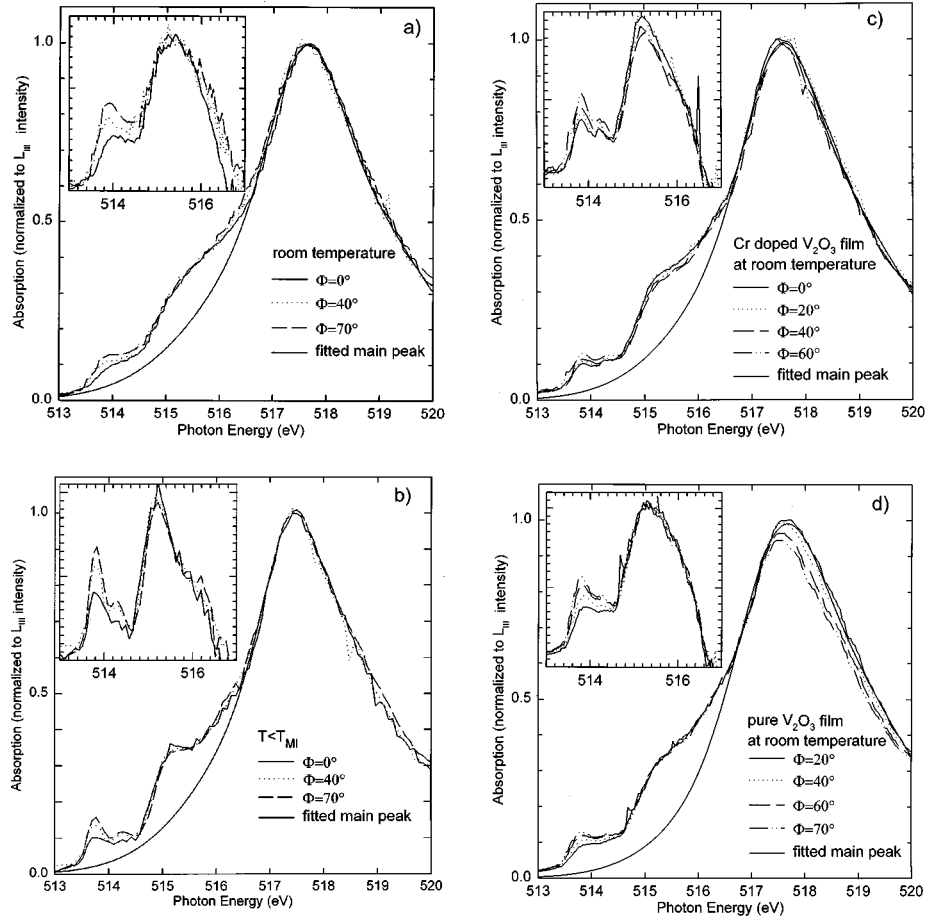


FIG. 3. The V L_{III} x-ray-absorption edge of various materials under different conditions. The inset shows the prepeak structure after subtraction of a fit to the main edge (solid line in each main figure). (a) is a (0001) single crystal of V_2O_3 at room temperature, i.e., in the metallic state. (b) is the same crystal below T_{MI} , in the insulating state. (c) is a Cr-doped insulating trigonal V_2O_3 thin film, while (d) is a pure insulating V_2O_3 thin film.

Fig. 3, to specific unoccupied initial states due to strong final state intra-atomic interactions,¹⁹ and we therefore focus on changes in the spectra. Comparison of Figs. 3(b) and 3(c) shows that the spectral features of the Cr-doped insulating phase are somewhat broader than those of the insulating phase of the pure V_2O_3 single crystal. Possible explanations include (a) the nonuniform stress (negative pressure) experienced by the thin film due to the film-substrate lattice mismatch,¹⁶ and (b) lattice distortions stemming from the substitution of Cr on V sites; alloys are expected to show broadening. The angular dependence increases in the insulating phase, although it is weaker than for the O $1s$ spectra. The low-energy peak does vary with angle, although less strongly than for the O $1s$ edge, and the higher-energy peaks change only slightly with angle. Nevertheless, the increase in angular anisotropy is likely due to the same cause as for the O $1s$ spectra, namely, an increase in the trigonal distortion of insulating compared to conducting phases. In contrast to the O $1s$ spectra, the lowest-energy V $2p$ feature shifts only about 0.15 eV at the MIT.

Most interestingly, comparison of Fig. 3(a) with Figs. 3(b), 3(c), and 3(d) shows that the features at the V $2p$ edge narrow considerably in the insulating phases relative to the metallic phase, both monoclinic (pure single crystal) and trigonal (pure and Cr-doped thin film). No such narrowing is observed (Figs. 1 and 2) in the O $1s$ spectra. The narrowing

occurs abruptly at T_{MI} in the single crystal and is observed in the other insulating phases already at room temperature, showing that it is a property of the insulating phase. We discuss three possible causes of such narrowing: (a) band narrowing (in the initial state), (b) an increase in the final state lifetime, and (c) a change in the electron-lattice interaction.

Explanation (a), band narrowing, appears unlikely, since the white lines at the O $1s$ edge do not narrow at the MIT, and no band narrowing is observed in photoemission (Fig. 4), which exhibits broad features in the metallic as well as in the insulating state. In fact, detailed angular-resolved photoemission in the metallic and insulating phase of V_2O_3 (Refs. 20 and 22) show only slight dispersion of the bands close to ϵ_F and no change in the insulating phase, except for a shift of the bands (dominantly of V $3d$ character) to higher binding energies and the opening of a gap at ϵ_F . The lifetime of the $(n-1)$ -electron state created in photoemission therefore does not change in the insulating phase.

An increase in the n -electron final-state lifetime in the insulating state, explanation (b), could occur since a local electron-hole excitation, or exciton, is more likely to form in an insulator than in a metal. Recent inelastic x-ray scattering²¹ in fact suggests the formation of an exciton state in the insulating phase. Exciton formation is consistent with

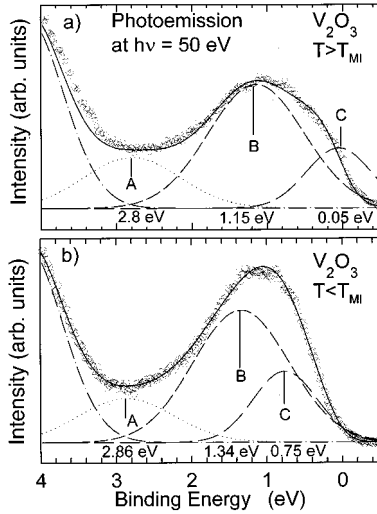


FIG. 4. Photoemission spectra of V_2O_3 , above and below the metal-insulator transition. The dotted curves are a three Gaussian fit to the spectra.

our measurements, showing that the lowest-energy L_{III} peak is ~ 0.15 eV lower in energy in the insulating phase than in the metallic phase; however, the next spectral peak does not similarly shift.

The third possible explanation, (c), a change in the role of electron-lattice coupling, is consistent with the photoemission data, which show dispersionless broad Gaussian features,^{20,22} and has been discussed by de Groot *et al.*²³ for the case of the O $1s$ edge in V_2O_5 . The Franck-Condon principle suggests how the $V 2p^{53}d^{n+1}$ final state could couple to vibrational modes and broaden features in the x-ray-absorption spectra. Interatomic distances are very sensitive to final-state occupancy, so promotion of an electron into an antibonding state in the x-ray-absorption process makes the equilibrium bond distance in the final state different from that in the initial state. As indicated schematically in Fig. 5, due to the difference in the equilibrium position between ground state and final state, excitation can occur into states with, due to the steep slope of the potential, a wide range of energies, and this is observed as spectral broadening. Since band-structure calculations⁴ imply V-V and O-O hybridization is much larger than interatomic V-O hybridization, V $2p$ absorption, which excites an electron into an antibonding d orbital, primarily affects the V-V potential. In the insulating phase, because the V-V distance is larger, the ground-state minimum is closer to the excited-state minimum than in the metallic phase. Therefore the insulating state will experience less Franck-Condon broadening, as observed. This explanation requires that the spectral width be temperature dependent, while within our experimental resolution we see no such temperature dependence, in either the O $1s$ or the V $2p$. The only observable width change occurs on entering the insulating phase. This could be due to the rather large Debye temperature of V_2O_3 ($\Theta_D = 580$ K),²⁴ well above the temperature range measured (< 400 K), so that little change in the occupied phonon density of states would be expected. The observed narrowing implies that electron-phonon coupling decreases in the insulating phase.

Two other observations support this explanation of the

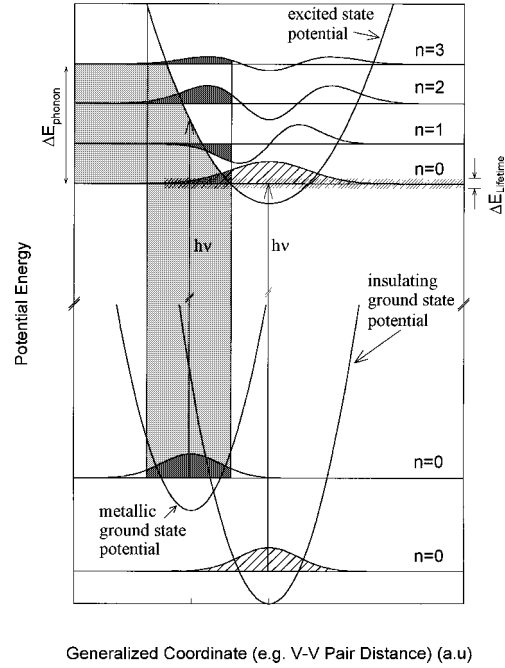


FIG. 5. Franck-Condon broadening in the insulating state, in which the ground-state potential minimum nearly overlaps the excited state potential minimum, resulting in little additional broadening beyond that due to the finite lifetime of the excited state, compared to the metallic state, in which the ground-state potential overlaps a rapidly varying portion of the excited state potential, so several vibrational states are accessible from the initial state, causing additional broadening.

broadening: (a) The V_2O_3 lattice is close to an instability, as indicated by the structural transitions it undergoes, so the lattice may be expected to be very sensitive to excitations into V $3d$ states; (b) the measured Gaussian line shape of the photoemission spectra, which is consistent with inhomogeneous broadening caused by the excitation of phonons in the photoemission process.^{20,22}

Figure 4 shows photoemission spectra, which reflect the occupied electronic states, of the V_2O_3 single crystal in the metallic and insulating phases. The spectra change markedly at the MIT, indicating that this transition takes place also in the surface region, since photoemission is more surface sensitive than x-ray absorption. To help quantify the changes seen, the spectra were fitted with several Gaussians, including the Fermi distribution in the metallic phase. To describe the occupied states within a few eV of ϵ_F it is necessary to include three Gaussians. Their resonance behavior as a function of photon energy implies that they are all due primarily to V $3d$ bands.^{20,22,25} Figure 4 shows that in the insulating phase peak B shifts about 0.2 eV to higher binding energy, while the peak nearest ϵ_F , peak C, shifts about 0.7 eV. Adding the latter shift (downward) to the slight upward shift of the unoccupied e_g^π and a_{1g} states observed in the x-ray absorption, we obtain a result consistent with optical measurements,^{26,27} although no final-state effects are taken into account, which may account for the fact that the shift of the V $2p$ is less. Unlike the V $2p$ edges, the photoemission features have the same width in the metallic and insulating phase.

In summary, we have used x-ray absorption and photo-

emission spectroscopy to show that, although they are structurally different, the electronic structure of trigonal pure and Cr-doped V₂O₃ thin films and low-temperature monoclinic insulating V₂O₃ is essentially the same, and all three differ in similar ways from metallic V₂O₃. This implies that the decisive factor in the MIT is not the symmetry breaking that brings about the monoclinic phase, but rather the increase in the *c/a* ratio, which causes increased distortion of the VO₆ octahedra. We observe narrowing of V 3*p* x-ray-absorption features in insulating phases compared to the metallic phase,

which we attribute to Franck-Condon-enhanced contribution of lattice degrees of freedom in the metallic phase.

ACKNOWLEDGMENTS

This project was supported by BMBF Contract No. 05 60 5 WAA and by the U.S. Department of Energy Division of Chemical Sciences Contract No. DE-FG02-96ER14660. The NSLS is supported by the DOE Divisions of Materials and Chemical Sciences.

-
- ¹P. D. Dernier, and M. Marezio, *Phys. Rev. B* **2**, 3771 (1970).
²J. B. Goodenough, in *Proceedings of the Tenth International Conference on the Physics of Semiconductors* (U.S. Atomic Energy Commission, Oak Ridge, 1970), p. 304; *Prog. Solid State Chem.* **5**, 145 (1972).
³G. W. Rathenau, and J. B. Goodenough, *J. Appl. Phys.* **39**, 403 (1968).
⁴L. F. Mattheis, *J. Phys.: Condens. Matter* **6**, 6477 (1994).
⁵G. Sawatzky, and D. Post, *Phys. Rev. B* **20**, 1546 (1979); N. Beatham, A. F. Orchard, and G. Thornton, *J. Phys. Chem. Solids* **42**, 1051 (1981).
⁶R. L. Kurtz, and V. E. Henrich, *Phys. Rev. B* **28**, 6699 (1983); J. M. McKay, M. H. Mohamed, and V. E. Henrich, *ibid.* **35**, 4304 (1987).
⁷E. Goering, M. Schramme, O. Müller, R. Barth, H. Paulin, M. Klemm, M. L. denBoer, and S. Horn, *Phys. Rev. B* **55**, 4225 (1997).
⁸K. E. Smith, and V. E. Henrich, *Surf. Sci.* **225**, 47 (1990).
⁹K. E. Smith, J. L. Mackay, and V. E. Henrich, *Phys. Rev. B* **35**, 5822 (1987).
¹⁰K. E. Smith, and V. E. Henrich, *Phys. Rev. B* **38**, 5965 (1988).
¹¹J. Ashkenazi, and T. Chuchen, *Philos. Mag.* **32**, 763 (1975); J. Ashkenazi and M. Weger, *J. Phys. (Paris), Colloq.* **37**, C4-189 (1976).
¹²K. E. Smith, and V. E. Henrich, *Phys. Rev. B* **38**, 9571 (1988).
¹³K. E. Smith, and V. E. Henrich, *Phys. Rev. B* **50**, 1382 (1990).
¹⁴F. M. F. de Groot, *J. Electron Spectrosc. Relat. Phenom.* **62**, 111 (1993).
¹⁵F. M. F. de Groot, M. Grioni, J. C. Fuggle, J. Ghijsen, A. Sawatzky, and H. Petersen, *Phys. Rev. B* **40**, 5715 (1989).
¹⁶H. Schuler, G. Weissmann, C. Renner, S. Six, S. Klimm, F. Simmet, and S. Horn, in *Epitaxial Oxide Thin Films II*, edited by D. K. Fork *et al.*, MRS Soc. Symp. Proc. No. 401 (Materials Research Society, Pittsburgh, 1996); p. 61; H. Schuler, G. Weissmann, S. Klimm, and S. Horn, *Thin Solid Films* **299**, 119 (1997); H. Schuler, S. Klimm, and S. Horn (to be published).
¹⁷T. M. Rice, H. Launois, and J. P. Pouget, *Phys. Rev. Lett.* **73**, 22 (1994); **73**, 3042 (1994).
¹⁸A. I. Frenkel, E. A. Stern, and F. A. Chudnovsky, *Solid State Commun.* **102**, 637 (1997).
¹⁹F. M. F. de Groot, J. C. Fuggle, B. T. Thole, and G. A. Sawatzky, *Phys. Rev. B* **41**, 928 (1990).
²⁰E. Goering, M. Schramme, O. Müller, H. Paulin, M. Klemm, M. L. denBoer, and S. Horn, *Physica B* **230–232**, 996 (1997).
²¹E. D. Isaacs, P. M. Platzman, P. Metcalf, and J. M. Honig, *Phys. Rev. Lett.* **76**, 4211 (1996).
²²E. Goering, Ph.D. Thesis, University of Augsburg, 1996.
²³F. M. F. de Groot, J. C. Fuggle, B. T. Thole, and G. A. Sawatzky, *Phys. Rev. B* **41**, 928 (1990).
²⁴L. W. Wenger, and P. H. Keeson, *Phys. Rev. B* **15**, 5288 (1975).
²⁵S. Shin, S. Suga, M. Tanichugi, M. Fujisawa, H. Kanzaki, A. Fujimori, H. Daimon, Y. Ueda, K. Kosuge, and S. Kachi, *Phys. Rev. B* **41**, 4993 (1990).
²⁶G. A. Thomas, D. H. Rapkine, S. A. Carter, A. J. Millis, T. F. Rosenbaum, P. Metcalf, and J. M. Honig, *Phys. Rev. Lett.* **73**, 1529 (1994).
²⁷C. Renner, Diploma thesis, University of Augsburg, 1995.